

A NEW TRIPLE-BAND CPW-FED MONOPOLE ANTENNA FOR WLAN AND WIMAX APPLICATIONS

Y.-Y. Cui, Y.-Q. Sun, H.-C. Yang, C.-L. Ruan

Institute of Applied Physics
University of Electronic Science and Technology of China
Chengdu 610054, China

Abstract—A new CPW-fed antenna with triple-band is presented for simultaneously satisfying wireless local area network (WLAN) and world interoperability for microwave access (WiMAX) applications. The investigated antenna consists of a T-shaped monopole with a trapeziform ground plane and two parasitic elements to generate triple-band. The design methodology is outlined and the overall size is $32 \times 15 \times 1 \text{ mm}^3$. This antenna was numerically designed using Ansoft HFSS simulation software package. The measured 10 dB bandwidth for return loss is from 2.35 to 2.71 GHz and 3.35 to 3.72 GHz and 4.9 to 6.1 GHz, covering all the 2.4/5.2/5.8 GHz WLAN bands and 2.5/3.5/5.5 GHz WiMAX bands.

1. INTRODUCTION

Since the FCC announced to allow the unlicensed use of the ISM frequencies by any potential users, the wireless communications community has seen an enormous opportunity to drive many wireless devices that could communicate over short distances. Recently the multi-band or broadband antennas have attracted high interest for application to multimode communication systems [1–7]. The planar monopole antenna is a good candidate for wireless communication because of its simple structure, omni-directional radiation characteristic, low profile, and lightweight internal antenna. There are many studies of WLAN antennas for 2.4 GHz (2.4–2.484 GHz) and 5.2/5.8 GHz (5.15–5.35 GHz/5.725–5.825 GHz) bands were published [8–16]. The key design configurations in order to meet this multi-band operation include a monopole antenna fed with a meandered coplanar waveguide (CPW) [8], a CPW-fed tapered bent folded monopole with two resonant paths [9], a CPW-fed

monopole antenna [10], a microstrip-fed double-T monopole antenna [11]. A CPW-fed notched monopole antenna [12], a CPW-fed meander monopole antenna [13, 14], a novel planar monopole antenna with an H-shaped ground plane [15], a microstrip fed monopole patch antenna with three stubs [16]. From these studies, however, it can be observed that none of above-mentioned designs support the worldwide interoperability for microwave access (WiMAX) applications and achieve a multi-band response to cover the 2.5/3.5/5.5 GHz (2500–2690/3400–3690/5250–5850 MHz) WiMAX bands [17]. In this article, we propose a new CPW-fed monopole antenna for the purpose of WLAN/WiMAX operation. The antenna is originally designed as a T-shaped CPW-fed monopole with a trapeziform ground plane and two parasitic elements to generate the resonant responses. This way, the antenna can achieve a tri-band performance to simultaneously cover the most commonly used WLAN and WiMAX bands. The 10-dB bandwidth of simulated return losses reaches 2.35–2.71 GHz, 3.35–3.72 GHz and 4.9–6.1 GHz in the three bands, respectively, and can cover the 2.4–2.484 GHz, 5.15–5.35 GHz, and 5.725–5.825 GHz WLAN bands, and the 2.5–2.69 GHz, 3.4–3.69 GHz, and 5.25–5.85 GHz WiMAX bands.

2. ANTENNA CONFIGURATION

Fig. 1 illustrates the geometry and dimension of the proposed tri-band antenna for WLAN/WiMAX dual-mode operation. The antenna is composed of a T-shaped CPW line, where the signal strip is protruded with a length $L = 32$ mm to form monopole, with a trapeziform ground plane to broaden bandwidth and two parasitic strips (strip 1 and strip 2) placed together to form bends. These parasitic elements are placed asymmetrically on both sides of the monopole with a bend angle. The strip 1 has a length of $L_l + r_1$, where L_l is the length of the straight section of the strip 1 and r_1 is the length of the bent section, determined by s_1, s_3 in the present design. The strip 2 has a length of $L_r + r_2$, where L_r is the length of the straight section of the strip 2 and r_2 is the length of the bent section, determined by s_2, s_4 in the present design. The straight section have a same width $W_f = 2.4$ mm. The antenna was implemented on a inexpensive FR4 substrate with thickness of 1 mm and relative permittivity of 4.4. The CPW line has a signal strip of $W = 3.3$ mm and a gap of $g = 0.5$ mm to have a characteristic impedance of 50Ω . The spacing between parasitic strips and the monopole is s_1 and s_2 and the spacing between the parasitic strips and the ground is s_3 and s_4 , respectively. The printed monopole length determines the lowest resonant frequency while its

width affects the antenna resistance at the resonant frequency. The two parasitic elements generate the median and the highest resonant frequency, respectively.

3. SIMULATION RESULTS AND DISCUSSION

In this section, we present numerical results of the parametric studies for the proposed antenna, as show in Fig. 1. The results obtained are presented for the return losses as a function of frequency and the antenna performance is analyzed using high-frequency structure simulator (HFSS) [18].

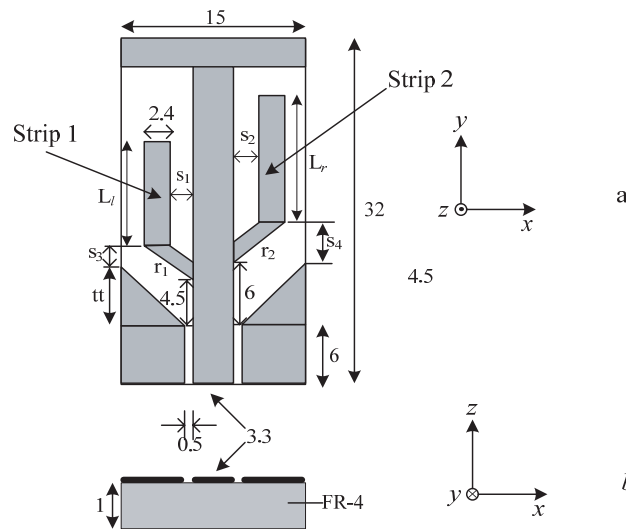


Figure 1. Geometry and dimension of the proposed antenna (in mm) a. top view b. cross-sectional view.

In the proposed antenna, the length of the monopole can be adjusted around quarter of a wavelength ($L = 32$ mm) to provide the fundamental resonant radiation band at 2.5 GHz. With a trapeziform ground plane, the bandwidth of the proposed antenna can effectively improved compared to a conventional rectangular ground plane. Here the trapeziform ground plane has three functions: the first is a ground plane for the monopole and the CPW; the second is as a radiating element; and the third is a component to form the distributed matching network with the monopole, which results in the wideband impedance characteristics compared to the conventional rectangular ground plane. Fig. 2 shows the simulated return loss of the antenna with a trapeziform

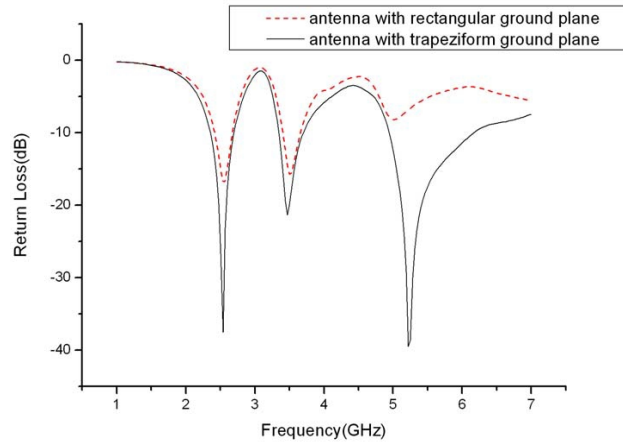


Figure 2. Comparison between antenna with rectangular ground plane and antenna with trapeziform ground plane.

ground plane and with a rectangular ground plane. It is found that with a trapeziform ground plane the impedance bandwidth of the highest resonant frequency is significantly increased and the return loss of the proposed antenna is also improved greatly. The band broadening can be optimized with choosing the $tt = 6$ mm.

The second and the third frequency are governed by the length L_l and L_r , respectively. The parameters s_1, s_2, s_3 and s_4 add a capacitive coupling to the antenna, which can broaden the bandwidth of the proposed antenna. The T-shaped monopole and the parasitic strips form a coupled system so that the size of one also influences the resonant frequencies of the other. By choosing proper parameter, we can realize a tri-band operation.

Fig. 3 shows the simulated return losses of the proposed antenna as a function of frequency for different values of L_l , and with $s_1 = 0.5$ mm, $s_2 = 1$ mm, $s_3 = 2$ mm, $s_4 = 3.5$ mm, $L_r = 11.5$ mm, $tt = 6$ mm. The figure shows that as L_l decreases, a good coupling is achieved for the highest resonant frequency, whereas the coupling of the lowest and median frequency are very slightly affected. The best performance is obtained when L_l about 6.5 mm.

Fig. 4 shows the simulated return losses of the proposed antenna as a function of frequency for different values of L_r , and with $s_1 = 0.5$ mm, $s_2 = 1$ mm, $s_3 = 2$ mm, $s_4 = 3.5$ mm, $L_l = 6.5$ mm, $tt = 6$ mm. It can be observed that the strip 2 corresponds to the median resonant frequency, which decreases as the length of the strip 2 increases. The widest bandwidth is achieved when L_r is around 11.5 mm.

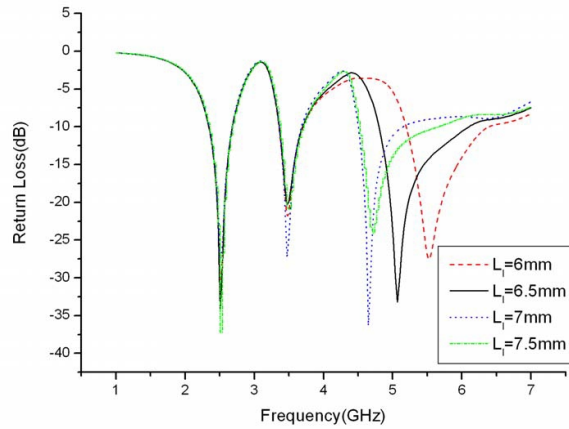


Figure 3. Simulated return loss with $s_1 = 0.5$ mm, $s_2 = 1$ mm, $s_3 = 2$ mm, $s_4 = 3.5$ mm, $L_r = 11.5$ mm, $tt = 6$ mm.

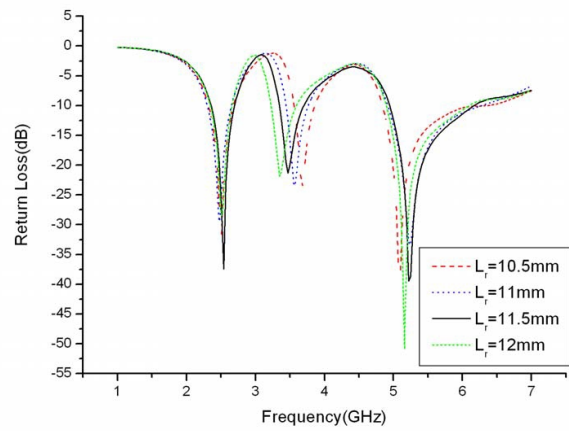


Figure 4. Simulated return loss with $s_1 = 0.5$ mm, $s_2 = 1$ mm, $s_3 = 2$ mm, $s_4 = 3.5$ mm, $L_l = 6.5$ mm, $tt = 6$ mm.

Fig. 5 illustrates the simulated return losses of the proposed antenna as a function of frequency for different values of s_1 , and with $L_l = 6.5$ mm, $L_r = 11.5$ mm, $s_2 = 1$ mm, $s_3 = 2$ mm, $s_4 = 3.5$ mm, $tt = 6$ mm. It can be seen from the figure that the space between strip 1 and monopole influences mainly the highest resonant frequency, and the best coupling is obtained when $s_1 = 0.5$ mm.

Fig. 6 exhibits the simulated return losses of the proposed antenna

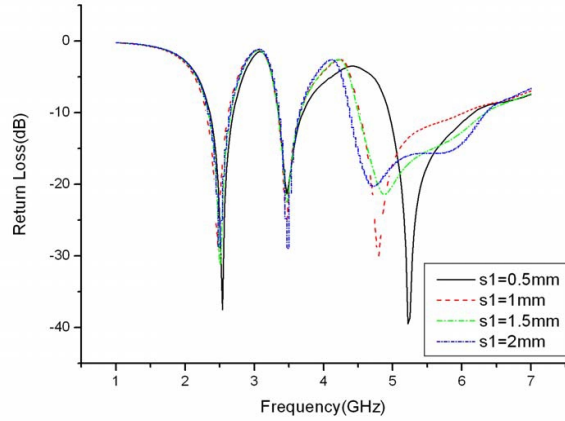


Figure 5. Simulated return loss with $L_l = 6.5$ mm, $L_r = 11.5$ mm, $s_2 = 0.5$ mm, $s_3 = 2$ mm, $s_4 = 3.5$ mm, $tt = 6$ mm.

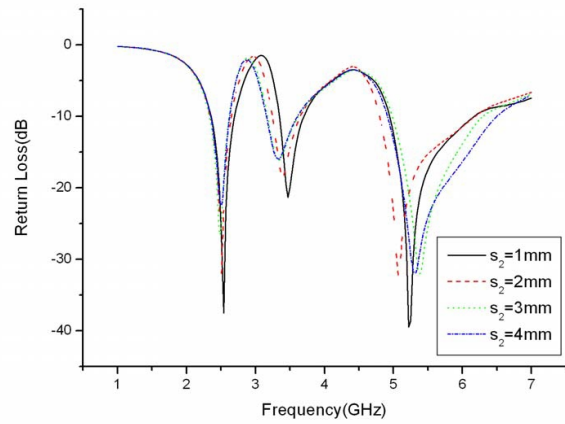


Figure 6. Simulated return loss with $L_l = 6.5$ mm, $L_r = 11.5$ mm, $s_1 = 0.5$ mm, $s_3 = 2$ mm, $s_4 = 3.5$ mm, $tt = 6$ mm.

as a function of frequency for different values of s_2 , and with $L_l = 6.5$ mm, $L_r = 11.5$ mm, $s_1 = 0.5$ mm, $s_3 = 2$ mm, $s_4 = 3.5$ mm, $tt = 6$ mm. It can be seen from the figure that the space between strip 2 and monopole influences mainly the median resonant frequency, and the best coupling is obtained when $s_2 = 1$ mm.

The effect of the distance between the parasitic strips and the ground plane is presented in Fig. 7 and Fig. 8. It indicates from

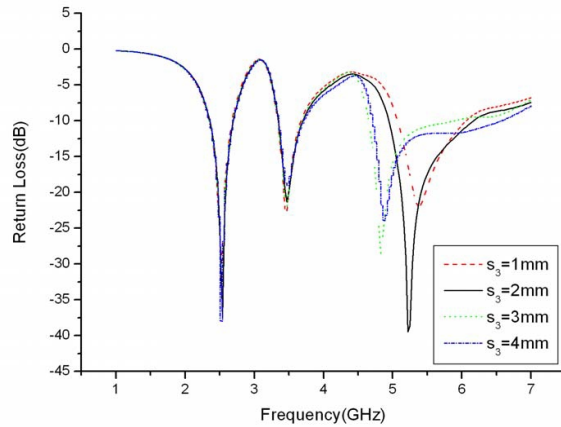


Figure 7. Simulated return loss with $L_l = 6.5$ mm, $L_r = 11.5$ mm, $s_1 = 0.5$ mm, $s_2 = 1$ mm, $s_4 = 3.5$ mm, $tt = 6$ mm.

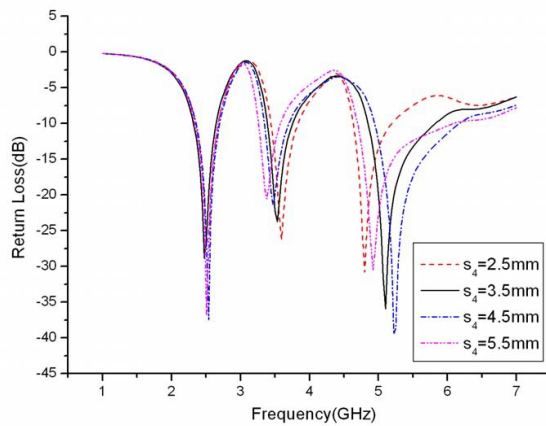
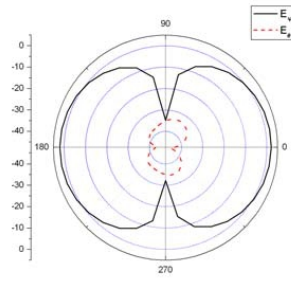
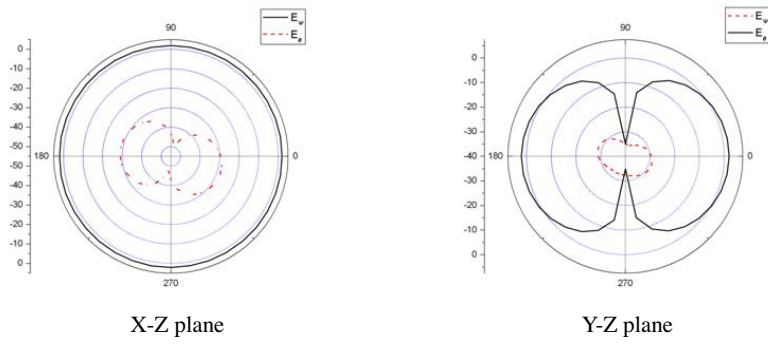


Figure 8. Simulated return loss with $L_l = 6.5$ mm, $L_r = 11.5$ mm, $s_1 = 0.5$ mm, $s_2 = 1$ mm, $s_3 = 2$ mm, $tt = 6$ mm.

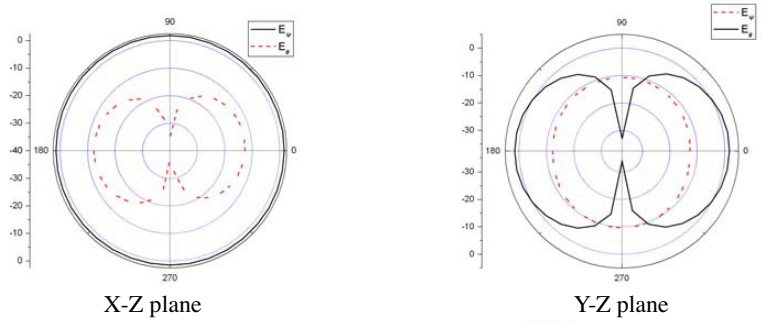
Fig. 7 that s_3 influences mainly the coupling of the highest resonant frequency, and the best coupling is obtained when s_3 is about 2 mm. In Fig. 8, it is observed that as s_4 varies, both the median and the highest frequency are affected. The optimal value is $s_4 = 3.5$ mm.

The simulated radiation pattern at 2.5, 3.5 and 5.5 GHz on the XZ -plane, YZ -plane and XY -plane are shown in Figure 9, respectively. Comparable electric components on the XZ, YZ and



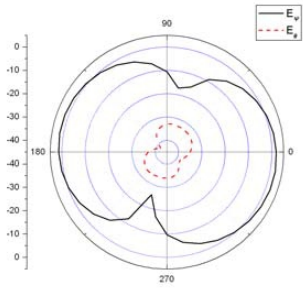
X-Y plane

(a)



X-Z plane

Y-Z plane



X-Y plane

(b)

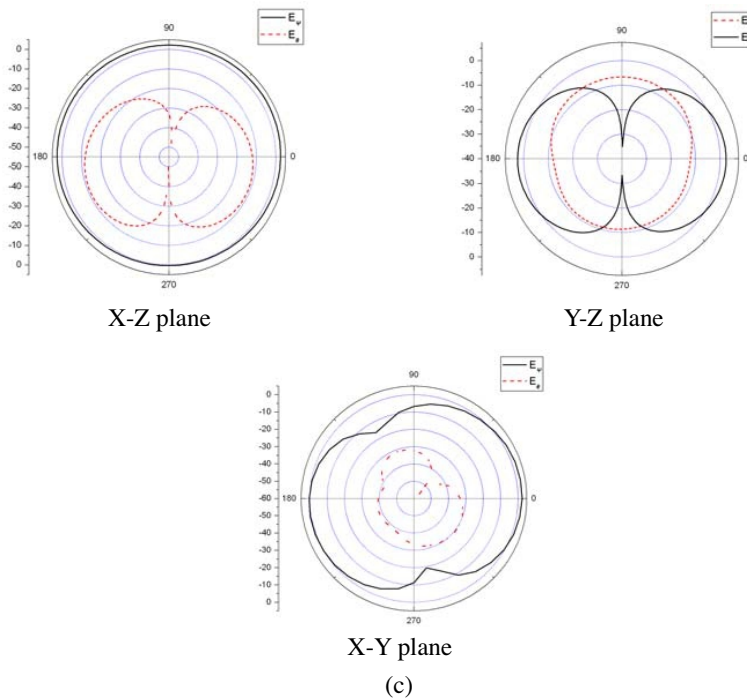


Figure 9. Simulated radiation patterns of the proposed antenna at (a) 2.5; (b) 3.5; and (c) 5.5 GHz.

XY planes are observed from these radiation patterns. This characteristic is advantageous for practical applications, because the propagation environment for wireless communications applications is usually very complex. The simulated antenna peak gain at operating frequencies 2.5 GHz, 3.5 GHz, and 5.5 GHz are 1.62 dB, 1.88 dB, 2.73 dB, respectively.

4. CONCLUSIONS

A new CPW-fed T-shaped monopole antenna with a trapeziform ground plane and two parasitic elements for WLAN/WiMAX dual-mode operation has been presented. The use of trapeziform ground plane and parasitic elements has generated different resonant frequency very remarkably to sufficiently cover the 2.4/5.2/5.8 GHz WLAN bands and 2.5/3.5/5.5 GHz WiMAX bands.

REFERENCES

1. Elsadek, H. and D. Nashaat, "Ultra miniturized E-shaped dual band PIFA on cheap foam and FR4 substrates," *Journal of Electromagnetic Waves and Applications*, Vol. 20, No. 3, 291–300, 2006.
2. Qin, W., "A novel patch antenna with a T-shaped parasitic strip for 2.4/5.8 GHz WLAN applications," *Journal of Electromagnetic Waves and Applications*, Vol. 21, No. 15, 2311–2320, 2007.
3. Zhang, G.-M., B. He, J. Liu, and J.-X. Zhu, "Novel multi-frequency and broad-band designs of isosceles triangular microstrip antennas with five stubs," *Journal of Electromagnetic Waves and Applications*, Vol. 21, No. 15, 2257–2266, 2007.
4. Congiu, S. and G. Mazzarella, "A tri-band printed antenna based on a sierpinski gasket," *Journal of Electromagnetic Waves and Applications*, Vol. 21, No. 15, 2187–2200, 2007.
5. Zhang, G.-M., J.-S. Hong, B.-Z. Wang, Q.-Y. Qin, L. Peng, and D.-M. Wan, "Novel dual-band and broad-band designs of circle slot antenna with a cross-shaped stub," *Journal of Electromagnetic Waves and Applications*, Vol. 21, No. 14, 2169–2179, 2007.
6. Liu, W.-C. and Y.-T. Kao, "CPW-fed compact meandered strip antenna on a soft substrate for dualband WLAN communication," *Journal of Electromagnetic Waves and Applications*, Vol. 21, No. 7, 987–995, 2007.
7. Liu, W.-C., "Miniaturized asymmetrical CPW-fed meandered strip antenna for triple-band operation," *Journal of Electromagnetic Waves and Applications*, Vol. 21, No. 8, 1089–1097, 2007.
8. Liu, W. C. and W. R. Chen, "CPW-fed compact meandered patch antenna for dual-band operation," *Electron. Lett.*, Vol. 40, No. 18, 1094–1095, Sep. 2004.
9. Kim, T. H. and D. C. Park, "CPW-fed compact monopole antenna for dual-band WLAN applications," *Electron. Lett.*, Vol. 41, No. 6, 292–293, Mar. 2005.
10. Lin, Y.-D. and P.-L. Chi, "Tapered bent folded monopole for dual-band wireless local area network (WLAN) systems," *IEEE Antenna Wireless Propag. Lett.*, Vol. 4, 355–357, 2005.
11. Kuo, Y.-L. and K.-L. Wong, "Printed double-T monopole antenna for 2.4/5.2 GHz dual-band WLAN operations," *IEEE Trans. Antennas Propag.*, Vol. 51, No. 9, 2187–2192, Sep. 2003. *Propag. Soc. Int. Symp. Dig.*, Vol. 1, 261–264, 2004.
12. Liu, W.-C., "CPW-fed notched monopole antenna for

- UMTS/IMT-2000/WLAN applications,” *Journal of Electromagnetic Waves and Applications*, Vol. 21, No. 6, 841–851, 2007.
13. Liu, W.-C., “Miniaturized asymmetrical CPW-fed meandered strip antenna for triple-band operation,” *Journal of Electromagnetic Waves and Applications*, Vol. 21, No. 8, 1089–1097, 2007.
 14. Fu, F. Y., L. P. Yan, K. Huang, and J. S. Dong, “Design and implement of a CPW-fed meander monopole antenna with V-shape notched ground for WLAN,” *Journal of Electromagnetic Waves and Applications*, Vol. 21, No. 14, 2129–2136, 2007.
 15. Zhang, G.-M., J.-S. Hong, B.-Z. Wang, Q.-Y. Qin, B. He and D.-M. Wan, “A novel planar monopole antenna with an H-shaped ground plane for dual-band WLAN applications,” *Journal of Electromagnetic Waves and Applications*, Vol. 21, No. 15, 2229–2239, 2007.
 16. Peng, L. and C.-L. Ruan, “A microstrip fed monopole patch antenna with three stubs for dual-band WLAN applications,” *Journal of Electromagnetic Waves and Applications*, Vol. 21, No. 15, 2359–2369, 2007.
 17. Deploying License-Exempt WiMAX Solutions Intel Corp. Santa Clara, CA, 2005 [Online].
 18. Ansoft High Frequency Structure Simulator (HFSS), Ver. 10.0, Ansoft Corporation.